



Published in final edited form as:

*Leukemia*. 2014 April ; 28(4): 961–964. doi:10.1038/leu.2014.21.

## Elucidation of the structural basis of interaction of the BCR-ABL kinase inhibitor, nilotinib (Tasigna®) with the human ABC drug transporter P-glycoprotein

Suneet Shukla<sup>†</sup>, Eduardo E. Chufan<sup>†</sup>, Satyakam Singh<sup>‡</sup>, Amanda P. Skoumbourdis<sup>||</sup>, Khyati Kapoor<sup>†</sup>, Matthew B. Boxer<sup>||</sup>, Damien Y. Duveau<sup>||</sup>, Craig J. Thomas<sup>||</sup>, Tanaji T. Talele<sup>‡</sup>, and Suresh V. Ambudkar<sup>†,\*</sup>

<sup>†</sup>Laboratory of Cell Biology, Center for Cancer Research, National Cancer Institute, NIH, Bethesda, MD 20892

<sup>‡</sup>Department of Pharmaceutical Sciences, College of Pharmacy and Health Sciences, St. John's University, Queens, NY 11439

<sup>||</sup>NIH Chemical Genomics Center, National Center for Advancing Translational Sciences, 9800 Medical Center Drive, Rockville, MD 20850

### Letter to the Editor

Nilotinib, imatinib (structures shown in Supplementary Figure S1) and other tyrosine kinase inhibitors (TKIs) have been shown to be transported by the ABC drug transporters P-glycoprotein (P-gp) and ABCG2 (1, 2). This is clinically important, as the transporters not only hamper the bioavailability of these TKIs but may also cause the emergence of drug resistance in patients. We have previously shown that imatinib and nilotinib interact at the substrate-binding pocket of ABC transporters, but do not interact at the ATP sites of these transporters (3). Identification of the key structural features of nilotinib and similar TKIs is essential for understanding their interaction with P-gp. Towards this goal, molecular docking, mutational mapping and quantitative structure-activity relationships were used to identify nilotinib's binding site on P-gp.

Nilotinib was docked in a human P-gp homology model that was developed based on the mouse P-gp crystal structure (4) using the XP-Glide docking method to understand the orientation and the complementarity of pharmacophore features of nilotinib with respect to the residues in the drug-binding pocket of P-gp (Figure 1a). Comparison of binding energy data for the docked poses of nilotinib at sites 1–4 (5) suggested site-1 (QZ59-RRR site) (4, 6) as the most favorable site (binding energy score of  $-9.52$  kcal/mol). The binding pocket is

Users may view, print, copy, download and text and data- mine the content in such documents, for the purposes of academic research, subject always to the full Conditions of use: [http://www.nature.com/authors/editorial\\_policies/license.html#terms](http://www.nature.com/authors/editorial_policies/license.html#terms)

Corresponding Author: Suresh V. Ambudkar, Laboratory of Cell Biology, NCI, NIH, 37 Convent Drive, Bethesda, MD 20892-4256, USA; Tel: 301-402-4178; Fax: 301-435-8188; [ambudkar@helix.nih.gov](mailto:ambudkar@helix.nih.gov).

Conflict-of-interest disclosure

The authors declare no competing financial interests.

SUPPLEMENTARY INFORMATION

Supplementary information is available at *Leukemia's* website.

lined by residues that form electrostatic and hydrophobic contacts with a pyridine, a pyrimidine, a methyl-substituted phenyl ring, the carbonyl oxygen atom of the amide linker and the trifluoromethylphenyl ring of nilotinib (Figure 1a). Among these, the Y307 residue showed significant interaction through hydrogen bonding to the pyridine ring (-N---HO-Y307, 2.4 Å) while A985 had hydrophobic contact with the CF<sub>3</sub> group (3.3 Å), phenyl ring (3.2 Å) and imidazole ring (4.1 Å) of nilotinib. Furthermore, M949 also showed hydrophobic contact with the imidazole ring (5.1 Å) of nilotinib, (highlighted in red in Figure 1a). Therefore, the residues (Y307, M949, and A985) that interact with three major functional groups (pyridine, CF<sub>3</sub> and imidazole) of nilotinib were selected for further analysis. The docking studies indicated these residues might determine the orientation and stabilization of nilotinib within the substrate-binding site of P-gp. These residues were mutated to Cys residues in a Cys-less P-gp to verify their role in interaction with nilotinib. Control Cys-less WT P-gp, Y307C, M949C and A985C P-gp mutants were expressed in HeLa cells (Supplementary Figure S2; mutants exhibited similar expression and function as Cys-less WT P-gp) and High-Five insect cells, as described in supplementary methods. Crude membranes from High-Five insect cells (expressing similar levels of mutant proteins (Figure 1b) were used to determine the interaction of these mutant P-gps with nilotinib. The effect of nilotinib was evaluated on ATPase activity and photolabeling of mutant P-gps with [<sup>125</sup>I]-IAAP binding (Figure 1c and Supplementary Table S1), as these approaches can be used to determine the interaction of substrates at the substrate-binding pocket of P-gp (7, 8). Nilotinib's ability to stimulate the ATPase activity of Y307C-, M949C- and A985C- mutant P-gps was significantly reduced or abolished compared to Cys-less WT P-gp (Supplementary Table 1). Similarly, nilotinib's ability to compete for [<sup>125</sup>I]-IAAP photolabeling was significantly reduced for Y307C- and almost completely lost for M949C- and A985C mutant P-gps (Figure 1c, Supplementary Table S1). These observations provided experimental support to the *in silico* docking studies. The residues Y307, M949 and A985 contribute to nilotinib binding, indicating that site-1 may be the primary binding site for nilotinib on P-gp. *In silico* introduction of these mutations in the homology model helped to visualize the local changes in the binding pocket (Supplementary Figure S3). In the nilotinib docked model of P-gp, pyridine nitrogen was present at a position 2.4 Å from the side chains of Y307; M949 was 5.1 Å from the imidazole ring, while A985 was 4.1 Å from the imidazole ring of nilotinib (Figure 1). In the triple mutant, the pyridine nitrogen atom lost one critical hydrogen bonding interaction with the Y307 residue, increasing the distance to 5.9 Å (Supplementary Figure S3). Similarly, the hydrophobic interactions with the imidazole ring and the trifluoro-methyl aniline moiety were lost when M949 and A985 were mutated to hydrophilic cysteine residue (Supplementary Figure S3). These data, taken together, provide clear evidence that site-1 is indeed the primary site of nilotinib binding on P-gp, with Y307 interacting with the pyridine ring, A985 interacting with the trifluoromethylphenyl group and M949 interacting with the imidazole ring of nilotinib.

To further validate the importance of functional groups of nilotinib for interacting with P-gp, five structural derivatives of nilotinib (Figure 2a) that lacked critical functional groups such as the pyridine ring, pyrimidine ring, CF<sub>3</sub> group and imidazole ring were synthesized (as described in Supplementary methods). These derivatives were evaluated for their interaction with P-gp by testing their ability to inhibit rhodamine 123 efflux from HeLa cells.

Compound **1** (CF<sub>3</sub> replaced by CH<sub>3</sub>) showed inhibition similar to that of nilotinib (data not shown), suggesting that substitution of fluorine with hydrogen at the CF<sub>3</sub> group is not a critical determinant of nilotinib's binding to the P-gp. Derivative **2** (no pyrimidine-pyridine ring system) was comparable to **3** (no pyridine ring) and **4** (imidazole replaced with a benzoic acid) was comparable to **5** (no imidazole ring) with respect to their ability to inhibit P-gp transport activity (data not shown). Therefore, **5** and **3**, derivatives lacking the key imidazole or pyridine/pyrimidine rings, respectively, were further tested for interaction with P-gp. Compared to nilotinib, **3** completely lost the ability to inhibit photolabeling of P-gp with [<sup>125</sup>I]-IAAP, but **5** was still able to inhibit approximately 30–35% of [<sup>125</sup>I]-IAAP photolabeling (Figure 2b, Supplementary Table S2). Similarly, **3** did not stimulate the ATPase activity but **5** was equally effective as nilotinib in stimulating the ATPase activity of Cys-less WT P-gp (Supplementary Table S3). In addition, **5** inhibited the rhodamine 123 efflux by P-gp, while **3** had no effect (Figure 2c). These results show that the interaction of nilotinib at the substrate-binding pocket of P-gp is significantly affected when the pyridine and/or pyrimidine ring is absent, while loss of the imidazole rings only slightly perturbs this interaction. Taken together, the results with derivatives corroborate the docking conformation and the mutational mapping data. While the pyridine and pyrimidine moieties of nilotinib are important for interaction at the drug-binding pocket, the imidazole group is not critical for this interaction.

Nilotinib and imatinib were also compared for their binding orientation in the substrate-binding pocket of P-gp (Supplementary Figure S4). As described in supplementary results, the observed affinity differences between nilotinib and imatinib for P-gp can be explained based on the above docking analysis and its comparison with the known crystal structures of imatinib and nilotinib bound to BCR-ABL kinase (9, 10).

Several studies have used a docking-based approach to identify the substrate-binding pocket in P-gp, but most of those studies relied on either SAR or mutagenesis alone [reviewed in (11)]. We used a two-pronged approach, where the docked orientation of nilotinib was not only validated by directed mutagenesis of selected residues but was also verified using the structural derivatives of nilotinib. Although the data derived from modeling and mutational studies with nilotinib and its derivatives corroborates well with the docked conformation of nilotinib, there is still a possibility that nilotinib may bind to a secondary site due to the chemical and structural flexibility of a large drug-binding pocket that can accommodate more than one ligand simultaneously (12–16).

In recent years, multidrug resistance-linked transporters have gained considerable attention as potential targets to improve cancer chemotherapy and to increase bioavailability/tissue penetration of drugs. Therefore, the interaction of these transporters with targeted therapeutic drugs such as nilotinib at the molecular level needs further elucidation. To our knowledge, this is the first report that provides an understanding of the interaction of nilotinib with human P-gp through molecular modeling, mutational mapping and SAR studies. We identified residues that are crucial for binding of nilotinib to the primary site on P-gp and by using derivatives we defined the molecular determinants of nilotinib for binding to P-gp. We believe these findings will help to synthesize novel inhibitors of TKs that do not

interact with P-gp, thus minimizing the possibility of development of resistance in cancer cells.

## Supplementary Material

Refer to Web version on PubMed Central for supplementary material.

## Acknowledgments

We thank Mr. George Leiman for editorial assistance.

### Funding Sources

This research was supported by the Intramural Research Program of the NIH, National Cancer Institute, Center for Cancer Research and National Center for Advancing Translational Sciences at the National Institutes of Health.

## References

1. Shukla S, Chen ZS, Ambudkar SV. Tyrosine kinase inhibitors as modulators of ABC transporter-mediated drug resistance. *Drug Resist Updat*. 2012; 15(1–2):70–80. Epub 2012/02/14. [PubMed: 22325423]
2. Brózik A, Hegedüs C, Erdei Z, Hegedüs T, Özvegy-Laczkó C, Szakács G, et al. Tyrosine kinase inhibitors as modulators of ATP binding cassette multidrug transporters: substrates, chemosensitizers or inducers of acquired multidrug resistance? *Expert Opin Drug Metab Toxicol*. 2011; 7(5):623–42. [PubMed: 21410427]
3. Shukla S, Sauna ZE, Ambudkar SV. Evidence for the interaction of imatinib at the transport-substrate site(s) of the multidrug-resistance-linked ABC drug transporters ABCB1 (P-glycoprotein) and ABCG2. *Leukemia*. 2008; 22(2):445–7. Epub 2007/08/11. [PubMed: 17690695]
4. Aller SG, Yu J, Ward A, Weng Y, Chittaboina S, Zhuo R, et al. Structure of P-Glycoprotein Reveals a Molecular Basis for Poly-Specific Drug Binding. *Science*. 2009; 323(5922):1718–22. [PubMed: 19325113]
5. Shi Z, Tiwari AK, Shukla S, Robey RW, Singh S, Kim IW, et al. Sildenafil reverses ABCB1- and ABCG2-mediated chemotherapeutic drug resistance. *Cancer Res*. 2011; 71(8):3029–41. Epub 2011/03/16. [PubMed: 21402712]
6. Tiwari AK, Sodani K, Dai C-I, Abuznait AH, Singh S, Xiao Z-J, et al. Nilotinib potentiates anticancer drug sensitivity in murine ABCB1-, ABCG2-, and ABCC10-multidrug resistance xenograft models. *Cancer Lett*. 2013; 328(2):307–17. [PubMed: 23063650]
7. Ambudkar SV, Dey S, Hrycyna CA, Ramachandra M, Pastan I, Gottesman MM. Biochemical, cellular, and pharmacological aspects of the multidrug transporter. *Annu Rev Pharmacol Toxicol*. 1999; 39:361–98. [PubMed: 10331089]
8. Sauna ZE, Ambudkar SV. About a switch: how P-glycoprotein (ABCB1) harnesses the energy of ATP binding and hydrolysis to do mechanical work. *Mol Cancer Ther*. 2007; 6(1):13–23. Epub 2007/01/24. [PubMed: 17237262]
9. Schindler T, Bornmann W, Pellicena P, Miller WT, Clarkson B, Kuriyan J. Structural mechanism for STI-571 inhibition of abelson tyrosine kinase. *Science*. 2000; 289(5486):1938–42. Epub 2000/09/16. [PubMed: 10988075]
10. Weisberg E, Manley P, Mestan J, Cowan-Jacob S, Ray A, Griffin JD. AMN107 (nilotinib): a novel and selective inhibitor of BCR-ABL. *Br J Cancer*. 2006; 94(12):1765–9. Epub 2006/05/25. [PubMed: 16721371]
11. Palmeira A, Sousa E, Vasconcelos MH, Pinto M, Fernandes MX. Structure and ligand-based design of P-glycoprotein inhibitors: a historical perspective. *Curr Pharm Des*. 2012; 18(27):4197–214. Epub 2012/07/26. [PubMed: 22827485]

12. Dey S, Ramachandra M, Pastan I, Gottesman MM, Ambudkar SV. Evidence for two nonidentical drug-interaction sites in the human P-glycoprotein. *Proc Natl Acad Sci U S A*. 1997; 94(20): 10594–9. [PubMed: 9380680]
13. Loo TW, Bartlett MC, Clarke DM. Simultaneous binding of two different drugs in the binding pocket of the human multidrug resistance P-glycoprotein. *J Biol Chem*. 2003; 278(41):39706–10. Epub 2003/08/12. [PubMed: 12909621]
14. Lugo MR, Sharom FJ. Interaction of LDS-751 and rhodamine 123 with P-glycoprotein: evidence for simultaneous binding of both drugs. *Biochemistry*. 2005; 44(42):14020–9. Epub 2005/10/19. [PubMed: 16229491]
15. Ambudkar SV, Kim IW, Sauna ZE. The power of the pump: mechanisms of action of P-glycoprotein (ABCB1). *Eur J Pharm Sci*. 2006; 27(5):392–400. Epub 2005/12/15. [PubMed: 16352426]
16. Marcoux J, Wang SC, Politis A, Reading E, Ma J, Biggin PC, et al. Mass spectrometry reveals synergistic effects of nucleotides, lipids, and drugs binding to a multidrug resistance efflux pump. *Proc Natl Acad Sci U S A*. 2013; 110(24):9704–9. Epub 2013/05/22. [PubMed: 23690617]

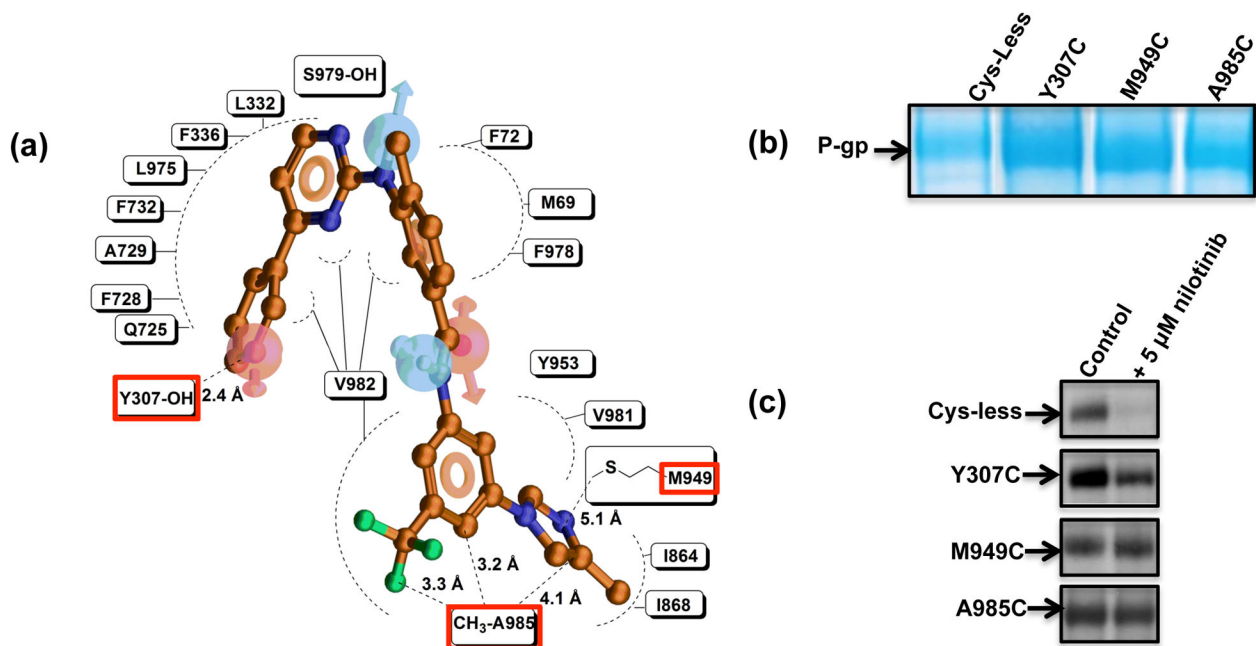


**Figure 1.**

Docking of nilotinib in the drug-binding pocket of human P-gp and analyses of mutant proteins. (a) Glide-predicted binding pocket of nilotinib in the homology model of human P-gp. Nilotinib was docked in a human P-gp homology model using Glide, as described in supplemental Materials and Methods. The amino acids that contribute to nilotinib's binding site are shown here. Three residues (Y307, M949 and A985) used for mutational analyses are highlighted by red boxes. The predicted distance of these residues from the closest functional group of nilotinib is marked. (b) Expression of mutant P-gps. Colloidal blue stain of crude membrane protein (10  $\mu$ g/lane) from Cys-less WT-P-gp, Y307C, M949C and A985C P-gps expressed in High-Five insect cells. (c) Nilotinib does not inhibit the labeling of mutant P-gps with [ $^{125}$ I]-IAAP. A representative autoradiogram from three independent experiments with Cys-less WT, Y307C, M949C and A985C mutant P-gps photo-crosslinked with [ $^{125}$ I]-IAAP in the absence or presence of 5  $\mu$ M nilotinib is shown.

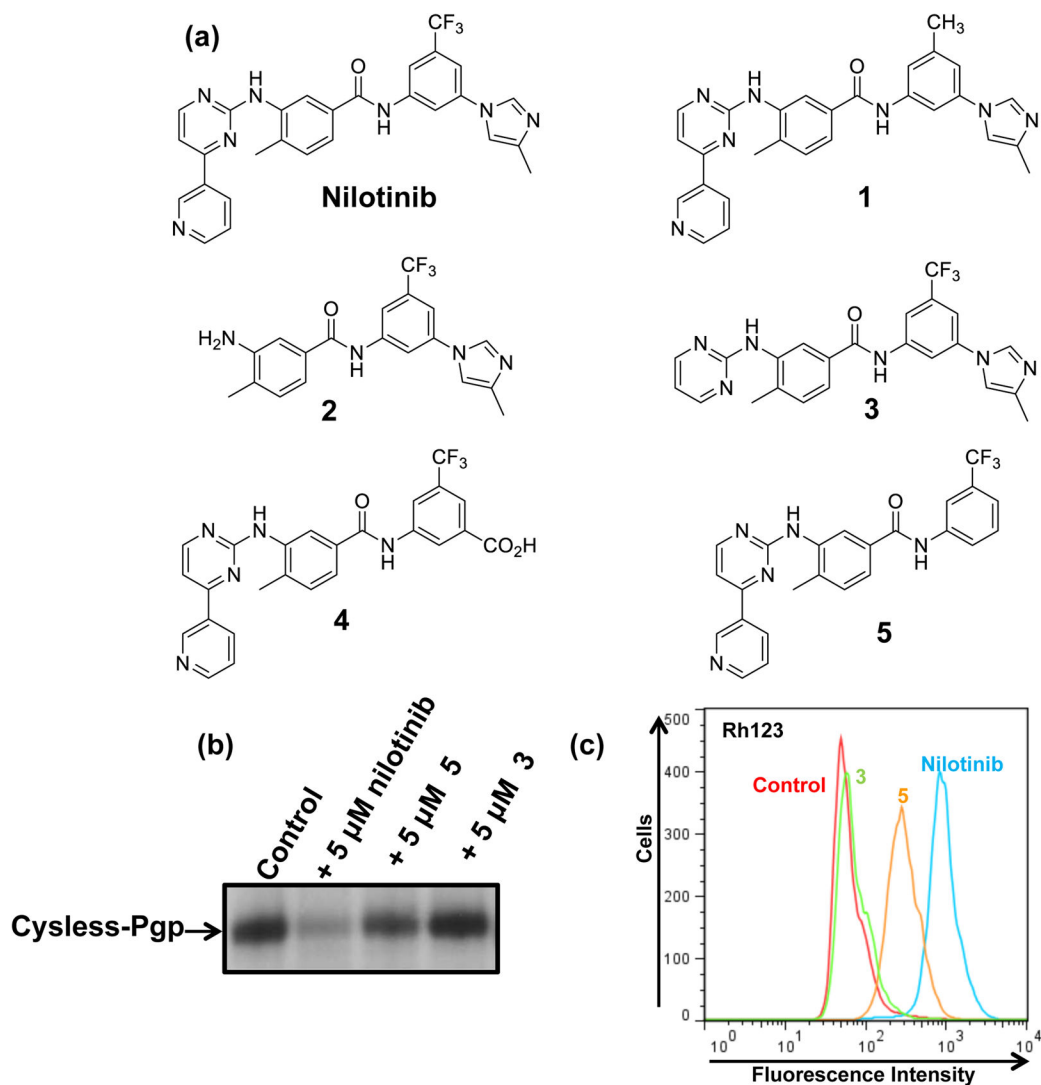


**Figure 2.** Synthesis of nilotinib derivatives and characterization of their interaction with P-gp. (a) Chemical structures of nilotinib and its derivatives used in this study. Nilotinib and derivatives **1**, **2**, **3**, **4** and **5** were synthesized as described in supplementary methods. (b) A representative autoradiogram from three independent experiments with Cys-less WT P-gps photo-crosslinked with [<sup>125</sup>I]-IAAP in the absence or presence of 5 μM nilotinib or derivative **3** and **5** is shown. (c) The histogram shows accumulation of rhodamine 123 in the presence and absence of 5 μM of nilotinib or derivative **3** or **5** in BacMam-P-gp virus-transduced HeLa cells (additional details are given in the legend to supplementary Figure S2)